HHS Public Access

Author manuscript

Anesthesiology. Author manuscript; available in PMC 2023 January 12.

Published in final edited form as:

Anesthesiology. 2021 February 01; 134(2): 234–247. doi:10.1097/ALN.0000000000003635.

Molecular Modification of Transient Receptor Potential Canonical 6 Channels Modulates Calcium Dyshomeostasis in a Mouse Model Relevant to Malignant Hyperthermia

Jose Rafael Lopez, M.D., Ph.D.,
Department of Molecular Biosciences, University of California at Davis, Davis, California; Department of Research, Mount Sinai Medical Center, Miami Beach, Florida

Arkady Uryash, M.D., Ph.D.,
Department of Neonatology, Mount Sinai Medical Center, Miami Beach, Florida

Jose Adams, M.D.,
Department of Neonatology, Mount Sinai Medical Center, Miami Beach, Florida

Philip M. Hopkins, M.D., F.R.C.A.,
Institute of Medical Research at St. James's University Hospital, University of Leeds, Leeds, United Kingdom

Paul D. Allen, M.D., Ph.D.
Department of Molecular Biosciences, University of California at Davis, Davis, California; Institute of Medical Research at St. James's University Hospital, University of Leeds, Leeds, United Kingdom

Abstract

Background: Pharmacologic modulation has previously shown that transient receptor potential canonical (TRPC) channels play an important role in the pathogenesis of malignant hyperthermia. This study tested the hypothesis that genetically suppressing the function of TRPC6 can partially ameliorate muscle cation dyshomeostasis and the response to halothane in a mouse model relevant to malignant hyperthermia.

Methods: This study examined the effect of overexpressing a muscle-specific nonconducting dominant-negative TRPC6 channel in 20 *RYR1*-p.R163C and 20 wild-type mice and an equal number of nonexpressing controls, using calcium- and sodium-selective microelectrodes and Western blots.

Results: *RYR1*-p.R163C mouse muscles have chronically elevated intracellular calcium and sodium levels compared to wild-type muscles. Transgenic expression of the nonconducting TRPC6 channel reduced intracellular calcium from 331 ± 34 nM (mean ± SD) to 190 ± 27

Correspondence Address correspondence to Dr. Allen: St. James's University Hospital, Leeds, LS9 7TF United Kingdom. p.d.allen@leeds.ac.uk.

Competing Interests
The authors declare no competing interests.

Supplemental Digital Content is available for this article.

nM ($P < 0.0001$) and sodium from 15 ± 1 mM to 11 ± 1 mM ($P < 0.0001$). Its expression lowered the increase in intracellular Ca^{2+} of the TRPC6-specific activator hyperforin in *RYR1*-p.R163C muscle fibers from 52% (348 ± 37 nM to 537 ± 70 nM) to 14% (185 ± 11 nM to 210 ± 44 nM). Western blot analysis of TRPC3 and TRPC6 expression showed the expected increase in TRPC6 caused by overexpression of its dominant-negative transgene and a compensatory increase in expression of TRPC3. Although expression of the muscle-specific dominant-negative TRPC6 was able to modulate the increase in intracellular calcium during halothane exposure and prolonged life (35 ± 5 min *vs.* 15 ± 3 min; $P < 0.0001$), a slow, steady increase in calcium began after 20 min of halothane exposure, which eventually led to death.

Conclusions: These data support previous findings that TRPC channels play an important role in causing the intracellular calcium and sodium dyshomeostasis associated with *RYR1* variants that are pathogenic for malignant hyperthermia. However, they also show that modulating TRPC channels alone is not sufficient to prevent the lethal effect of exposure to volatile anesthetic malignant hyperthermia–triggering agents.

Malignant hyperthermia (MH) is an autosomal dominant hypermetabolic condition triggered by volatile anesthetics, such as isoflurane and succinylcholine.[1-4] Molecular genetic studies have established the type 1 ryanodine receptor gene (*RYR1*) encoding the skeletal muscle sarcoplasmic reticulum Ca^{2+} release channel as the primary locus for both MH susceptibility and central core disease.[2-6] A common characteristic of muscle expressing MH-*RYR1* variants, both in patients[7] and in experimental models,[8-12] is an increased intracellular Ca^{2+} concentration compared to muscle from nonsusceptible subjects. In three experimental murine models of MH with variants in *RYR1* that are known to be pathogenic in humans, we have shown that exposure to halothane or isoflurane at clinically relevant concentrations causes intracellular Ca^{2+} concentration to rise several-fold in their muscles, whereas exposure to the same concentrations of halothane or isoflurane has no effect in muscles from mice without *RYR1* variants.[10-12] Previously, we introduced a new paradigm that implicates nonspecific sarcolemmal cation entry *via* transient receptor potential canonical (TRPC) channels both as the predominant source of acutely elevated intracellular Ca^{2+} and sodium concentration during fulminant MH and as important contributors to chronically elevated intracellular Ca^{2+} and sodium concentrations in quiescent MH-susceptible muscles.[13,14]

Our aim in this study was to use molecular methods in combination with pharmacologic agents to further test the primary hypothesis that TRPC3 and TRPC6 channels are directly responsible for the high intracellular Ca^{2+} concentration seen in resting MH-susceptible muscles, with a secondary hypothesis that blocking TRPC6 could prevent the massively elevated intracellular Ca^{2+} concentration observed during the MH crisis after exposure to triggering agents and subsequent death. We have done this using our *RYR1*-p.R163C knock-in murine model of MH[10] crossed with a transgenic animal overexpressing a dominant-negative nonconducting TRPC6 channel in their skeletal muscles.[15,16] This transgene exerts its effect by blocking the activity of TRPC6 and perhaps also by modulating TRPC3 because these two closely related TRPC channel isoforms are known to form heterotetramers at the plasma membrane.[17] In a previous study in two murine models of muscular dystrophy, expressing this nonconducting channel relieved their muscle pathology and restored muscle function to near normal levels.[15]

Materials and Methods

Animals

The animals used in this study were (1) wild-type C57BL/6J mice, (2) C57BL/6J knock-in mice heterozygous for the *RYR1* variant resulting in the amino acid change p.R163C in the RyR1 protein (R163C), (3) transgenic mice with skeletal muscle–specific overexpression of a nonconducting TRPC6 channel,[15] and (4) mice heterozygous for *RYR1*-p. R163C with skeletal muscle–specific expression of a nonconducting TRPC6 channel (the result of crossing *RYR1*-p. R163C with mice with skeletal muscle–specific expression of a nonconducting TRPC6 channel). The mice were used as close as possible to the time they achieved 3 months of age. In all, 91 mice (39 females and 52 males) were used as experimental animals. The animals for any phase of the study were chosen by their date of birth (oldest first) and their availability in the animal colony. All experimental procedures on animals were in accordance with the Care and Use Handbook of Laboratory Animals published by the U.S. National Institutes of Health (Bethesda, Maryland; publication No. 85-23, revised 1996) and approved by the Institutional Animal Care and Use Committees at the University of California at Davis, Davis, California; the Mount Sinai Hospital, Miami Beach, Florida, and the Home Office in the United Kingdom (London).

Experimental Preparations

The experiments were conducted (1) *in vitro* using single muscle fibers obtained by enzymatic digestion of flexor digitorum brevis muscles dissected from 3- to 5-month-old anesthetized mice killed by cervical dislocation;[18] with flexor digitorum brevis fibers used for measurements of intracellular ion concentrations 4 to 6 h after isolation; or (2) *in vivo* by measurement of intracellular ion concentrations in surgically exposed vastus lateralis fibers of mice anesthetized using a mixture of intraperitoneal ketamine (100 mg/kg) and xylazine (5 mg/kg).[13]

Ca^{2+}- and Sodium-selective Microelectrodes

Double-barreled Ca^{2+}- and sodium-selective microelectrodes were prepared and individually calibrated before and after the determination of intracellular calcium concentration or intracellular sodium concentration as described previously.[13,19] Only those Ca^{2+} selective microelectrodes with a linear relationship between one micromolar and one hundred nanomolar (Nernstian response, 30.5 milivolts per negative logarithm of the calcium concentration unit) or those sodium microelectrodes with Nernstian responses between 100 and 10 mM and a sub-Nernstian response (40 to 45 millivolts) between 1 and 10 mM were used experimentally. The sensitivity of the Ca^{2+}- and sodium-selective microelectrodes were not affected by any of the drugs used in the current study. After making measurements of resting intracellular free calcium concentration for $[Ca^{2+}]_r$ and resting intracellular sodium concentration for $[Na^+]_r$, all microelectrodes were recalibrated, and if the two calibration curves did not agree within 5 millivolts, data from that microelectrode were discarded. This resulted in the removal of the data of 11 animals from the final analysis.

Recording of Intracellular Ca^{2+} and Sodium in Muscle Fibers *In Vitro* and *In Vivo*

Intracellular Ca^{2+} and sodium determinations were performed *in vitro* on single flexor digitorum brevis muscle fibers as described previously[18] and *in vivo* on vastus lateralis fibers in anesthetized wild-type and *RYR1*-p.R163C mice.[10] The muscle fibers were impaled with double-barreled Ca^{2+}-selective or sodium-selective microelectrodes, and their potentials were recorded *via* a high-impedance amplifier (WPI Duo 773 electrometer; WPI, USA).[10] The data were not collected in any muscle cell whose membrane potential was less negative than minus 80 millivolts, and if that occurred at any time during the experiment, the data for that cell were not used for analysis.

The resting membrane potential from the 3 M KCl microelectrode was subtracted electronically from either the potential of the Ca^{2+} microelectrode or the sodium microelectrode to produce a differential Ca^{2+}-specific potential or sodium-specific potential that represents the intracellular Ca^{2+} or intracellular sodium concentrations, respectively. All voltage signals were stored in a computer for further analysis.

Solutions.—Normal Ringer solution contained 135 mM NaCl, 5 mM KCl, 1.8 mM $CaCl_2$, 1 mM $MgCl_2$, 18 mM $NaHCO_3$, 1.5 mM NaH_2PO, and 5 mM glucose, pH 7.2 to 7.3. 1-Oleoyl-2-acetyl-*sn*-glycerol, ethyl-1-(4-(2,3,3-trichloroacrylamide)phenyl)-5-(trifluoromethyl)-1H-pyrazole-4-carboxylate, and hyperforin solutions were made by adding the desired concentration of the reagent to normal Ringer solution. All *in vitro* experiments were performed at 37°C.

Halothane Survival Curve.—To investigate the effects of overexpressing a dominant-negative nonconducting TRPC6 in *RYR1*-p.R163C mice on the response to exposure to 2% halothane, we conducted a survival study on cohorts (7 mice per group) of 8- to 12-week-old wild-type, wild-type/dominant-negative TRPC6, *RYR1*-p.R163C, and *RYR1*-p.R163C/dominant-negative TRPC6 mice. Survival time was measured during an up to 60-min exposure to 2% halothane.

Western Blot Analysis of Protein Expression.—Gastrocnemius muscles from all genotypes were dissected, minced, and homogenized in modified radioimmunoassay precipitation assay buffer as described before.[20] Total protein concentration was determined using the Pierce BCA protein assay kit (ThermoFisher Scientific, USA). Proteins were separated on sodiumdodecylsulfate gel and transferred to nitrocellulose membrane. To avoid having errors added by attempting to measure all of the proteins on a single gel, by stripping the antibodies after making the first measurement, we performed the analysis by first slicing each membrane horizontally according to the molecular weight of proteins of interest. Each individual membrane strip was incubated with the primary anti-TRPC3, -TRPC6, and –glyceraldehyde-3-phosphate dehydrogenase antibodies based on the known protein size and protein standard markers. The levels of TRPC proteins were normalized to loading control using the housekeeping protein glyceraldehyde-3-phosphate dehydrogenase. Each strip from a single gel is shown as the example. Gels for each sample were run in triplicate and incubated with primary TRPC3, TRPC6, or glyceraldehyde-3-phosphate dehydrogenase followed by secondary fluorescent antibodies (Abcam, USA). All antibody

dilutions and signals were validated previously in our laboratory and by others.[14,21] Signals of the protein of interest were detected with Storm 860 fluorescent imaging system (GE Bio-Sciences, USA). Protein signals were quantified using MyImageAnalysis software (ThermoFisher Scientific), and the density of the TRPC proteins was normalized to the density of glyceraldehyde-3-phosphate dehydrogenase expression, which is thought not to be differentially expressed in these models.

Statistics

No specific power calculation was conducted before experimentation. The sample sizes used were based on our previous studies using other MH and non-MH animal models. Randomization methods were not used to assign the animals to be studied, and blinding of the investigators was not used. All values are expressed as means ± SD. Statistical analysis used two-tailed hypothesis testing. For studies done on muscle fibers both *in vitro* and *in vivo,* a one-way between-subjects ANOVA was performed with Tukey's posttest for multiple measurements to determine significance ($P < 0.05$). We used histograms (most commonly used graph to show frequency distributions) and the D'Agostino and Pearson test to assess the distribution of the data. Statistical analyses of Western blots were carried out using an unpaired Student's independent *t* test. To do this, we used an independent samples *t* test; namely, we compared two sample means from different populations regarding the same variable. The Mantel–Cox test was used to test for differences in survival between groups. All data collected were analyzed, and no outliers were removed from our analyses. Statistical analysis was done using GraphPad Prism 7.03 (GraphPad Software, Inc., USA). Data from 11 mice were discarded because of (1) the loss of microelectrode sensitivity to calcium detected by a drift of more than 5 millivolts between the first and the second microelectrode calibration curves in the range between pCa 6 and pCa 7; (2) broken microelectrode tips that did not allow us to carry out the postmeasurement calibration curves; and (3) the unexpected occurrence of electronic noise during the ion measurements that compromised the accuracy of the ion-specific voltage recorded.

Results

Intracellular Ca^{2+} and Sodium Concentrations in Muscle Fibers Expressing a Dominant-negative TRPC6 Channel

In vivo intracellular Ca^{2+} concentrations were 175% higher and intracellular sodium concentrations were 88% higher in *RYR1*-p.R163C vastus lateralis muscle fibers than those observed in wild-type muscle fibers ($P < 0.0001$; fig. 1). Expression of the dominant-negative TRPC6 reduced skeletal muscle intracellular Ca^{2+} and sodium concentrations in both wild-type and *RYR1*-p.R163C mice; however, the decreases caused by its expression were greater in *RYR1*-p.R163C/dominant-negative TRPC6 than in wild-type/dominant-negative TRPC6 mice (43% [$P < 0.0001$] *vs.* 21% [$P < 0.0001$] and 27% [$P < 0.001$] *vs.* 11% [$P = 0.002$] for intracellular Ca^{2+} and sodium concentrations, respectively; fig. 1). There were no differences in resting membrane potential among the four different genotypes. Similar differences in intracellular Ca^{2+} and sodium concentrations were observed *in vitro* in enzymatically isolated single flexor digitorum brevis muscle fibers (Supplemental Digital Content 1, http://links.lww.com/ALN/C515).

Expressing a Dominant-negative TRPC6 Channel in Skeletal Muscle Reduces the Elevation of Intracellular Ca^{2+} and Sodium Concentrations Elicited by 1-Oleoyl-2-acetyl-*sn*-glycerol

TRPC3/6 channels are directly activated by the ubiquitous intracellular second messenger diacylglycerol, whereas TRPC1/4/5 channels are not.[22] When we exposed single flexor digitorum brevis muscle fibers to the membrane-permeable diacylglycerol analog 1-oleoyl-2-acetyl-*sn*-glycerol[21,22] (100 μM) for 15 min, intracellular Ca^{2+} concentration increased in *RYR1*-p.R163C fibers by 132% ($P < 0.0001$), whereas in wild-type fibers, it increased by only 64% ($P < 0.0001$; fig. 2A). Similarly, 1-oleoyl-2-acetyl-*sn*-glycerol (100 μM) produced a greater elevation of intracellular sodium concentration in *RYR1*-p.R163C flexor digitorum brevis muscle fibers (70%, $P < 0.0001$) than in wild type (50%, $P < 0.0001$; fig. 2B). Similar results were obtained using 1,2-dioctanoyl-*sn*-glycerol, another membrane-permeable diacylglycerol analog[23] (Supplemental Digital Content 1, http://links.lww.com/ALN/C515). Expression of dominant-negative TRPC6 reduced the effect of 1-oleoyl-2-acetyl-*sn*-glycerol on both intracellular Ca^{2+} and sodium concentrations in both wild-type and *RYR1*-p.R163C flexor digitorum brevis muscle fibers (fig. 2, A and B).

Hyperforin-induced Elevation of Resting Intracellular Ca^{2+} Concentration

To demonstrate that the changes in intracellular Ca^{2} concentration seen with the expression of the dominant-negative nonconducting TRPC6 transgene were due to a reduction in the function of TRPC6, we measured intracellular Ca^{2+} concentration in single muscle fibers exposed to the TRPC6 activator hyperforin.[24] We have previously found that hyperforin caused a genotype-dependent rise in resting intracellular Ca^{2+} concentration in the *RYR1*-p. G2435R murine MH model.[14] Here, we found that exposure of wild-type and *RYR1*-p.R163C flexor digitorum brevis muscle fibers to 10 μM hyperforin produced a statistically significant increase in intracellular Ca^{2+} concentrations in both genotypes, but the effect was less marked in wild-type cells (34%, from 121 ± 2 nM to 162 ± 15 nM, $P = <0.001$) than in *RYR1*-p.R163C cells (54%, from 348 ± 37 nM to 537 ± 70 nM, $P = <0.001$; fig. 3). Expression of dominant-negative TRPC6 in flexor digitorum brevis muscle fibers markedly reduced the effect of hyperforin on intracellular Ca^{2+} concentration to only a 5% increase (from 94 ± 6 nM to 99 ± 6 nM; $P = 0.248$) in wild-type/dominant-negative TRPC6 fibers and a 14% increase in *RYR1*-p.R163C/dominant-negative TRPC6 fibers (from 185 ± 11 nM to 210 ± 43 nM; $P = 0.288$; fig. 3).

Ethyl-1-(4-(2,3,3-trichloroacrylamide)phenyl)-5-(trifluoromethyl)-1H-pyrazole-4-carboxylate Reduces Intracellular Ca^{2+} Concentration in RYR1-p.R163C/dominant-negative TRPC6 Skeletal Muscle Cells

The concept of functional specificity of Ca^{2+}-influx pathways was further explored by incubating single flexor digitorum brevis muscle fibers with the pyrazole compound ethyl-1-(4-(2,3,3-trichloroacrylamide)phenyl)-5-(trifluoromethyl)-1H-pyrazole-4-carboxylate, which is proposed to be a specific blocker of TRPC3.[25] Incubation with ethyl-1-(4-(2,3,3-trichloroacrylamide)phenyl)-5-(trifluoromethyl)-1H-pyrazole-4-carboxylate reduced intracellular Ca^{2+} concentration in *RYR1*-p.R163C flexor digitorum brevis muscle fibers from 353 ± 29 nM to 268

± 34 nM ($P < 0.0001$) and from 122 ± 3 nM to 108 ± 7 nM ($P < 0.001$) in wild type (fig. 4). Incubation with 10 μM ethyl-1-(4-(2,3,3-trichloroacrylamide)phenyl)-5-(trifluoromethyl)-1H-pyrazole-4-carboxylate almost normalized intracellular Ca^{2+} concentration in *RYR1*-p. R163C/dominant-negative TRPC6 fibers from 190 ± 15 nM to 130 ± 9 nM ($P < 0.0001$) and reduced intracellular Ca^{2+} concentration in wild-type/dominant-negative TRPC6 fibers from 93 ± 9 nM to 79 ± 8 nM ($P < 0.001$; fig. 4). In both wild-type and *RYR1*-p.R163C/dominant-negative TRPC6 genotypes, the percentage of reduction caused by ethyl-1-(4-(2,3,3-trichloroacrylamide) phenyl)-5-(trifluoromethyl)-1H-pyrazole-4-carboxylate was similar to the percentage of reduction seen after ethyl-1-(4-(2,3,3-trichloroacrylamide)phenyl)-5-(trifluoromethyl)-1H-pyrazole-4-carboxylate exposure in the absence of dominant-negative TRPC6 expression.

Expression of Dominant-negative TRPC6 Reduced the Increase of Intracellular Ca^{2+} Concentration in RYR1-p. R163C Muscle during Exposure to Halothane

Exposure to 2% halothane had no effect on intracellular Ca^{2+} concentration measured *in vivo* in the vastus lateralis fibers of wild-type mice but caused an immediate and statistically significant 273% elevation in intracellular Ca^{2+} concentration ($P < 0.0001$) in the vastus lateralis fibers of *RYR1*-p. R163C mice (fig. 5). Furthermore, all the *RYR1*-p.R163C animals succumbed to the MH crisis within 16 min of halothane exposure (fig. 6). Expression of dominant-negative TRPC6 in *RYR1*-p.R163C muscle, in addition to reducing intracellular Ca^{2+} concentration (fig. 5) before exposure to halothane, both statistically significantly attenuated the increase in intracellular Ca^{2+} concentration (125% *vs.* 275%; $P < 0.0001$) during exposure to halothane (fig. 5) and statistically significantly increased the survival time (fig. 6). The mean survival time of *RYR1*-p.R163C/dominant-negative TRPC6 mice was 35 ± 5 min (7 mice) *versus* 15 ± 3 min for *RYR1*-p.R163C mice (7 mice; $P < 0.0001$). However, dominant-negative TRPC6 expression was not sufficient to entirely prevent the elevation of intracellular Ca^{2+} concentration after halothane inhalation over time and did not prevent death as a result of the MH crisis. Figure 7 shows an experiment in which intracellular Ca^{2+} concentration and rectal temperature were recorded continuously *in vivo* in a *RYR1*-p.R163C/dominant-negative TRPC6 mouse until it succumbed to the MH crisis. Intracellular Ca^{2+} concentration rapidly increased from 236 to 465 nM immediately after exposure to halothane, remained between 422 to 498 nM for the next 14 to 18 min, and then increased slowly, reaching 900 to 1,000 nM after 34 min of halothane inhalation, when death occurred.

Effects of Ethyl-1-(4-(2,3,3-trichloroacrylamide) phenyl)-5-(trifluoromethyl)-1H-pyrazole-4-carboxylate in RYR1-p.R163C/dominant-negative TRPC6 Muscles during Exposure to Halothane

Although it was not possible to administer ethyl-1-(4-(2,3,3-trichloroacrylamide)phenyl)-5-(trifluoromethyl)-1H-pyrazole-4-carboxylate systemically, we were able to measure its local effects on skeletal muscle intracellular Ca^{2+} concentration *in vivo* by measuring intracellular Ca^{2+} concentration simultaneously in the left and right vastus lateralis muscles in wild-type/dominant-negative TRPC6 and *RYR1*-p.R163C/dominant-negative TRPC6 mice before and after exposure to 2% halothane. The left leg muscle was used as a control, whereas the right leg muscle was superfused continuously with 10 μM ethyl-1-(4-(2,3,3-

trichloroacrylamide)phenyl)-5-(trifluoromethyl)-1H-pyrazole-4-carboxylate for 15 min before and during the entire exposure to halothane. In the wild-type/dominant-negative TRPC6 left leg muscle, the intracellular Ca^{2+} concentration was 95 ± 4 nM, and this was unchanged after exposure to halothane (93 ± 5 nM; fig. 8A). Intracellular Ca^{2+} concentration was reduced to 84 ± 6 nM after 15 min of local incubation with 10 μM ethyl-1-(4-(2,3,3-trichloroacrylamide) phenyl)-5-(trifluoromethyl)-1H-pyrazole-4-carboxylate and as before was unaffected by exposure to 2% halothane (86 ± 6.2 nM; fig. 8A). In *RYR1*-p.R163C/dominant-negative TRPC6 muscle, basal intracellular Ca^{2+} concentration was 186 ± 20 nM and rose to 415 ± 29 nM immediately after exposure to 2% halothane (fig. 8B). Incubation with ethyl-1-(4-(2,3,3-trichloroacrylamide)phenyl)-5-(trifluoromethyl)-1H-pyrazole-4-carboxylate reduced basal intracellular Ca^{2+} concentration from 194 ± 11 nM to 146 ± 12 nM ($P < 0.0001$) and statistically significantly blunted the increase seen after exposure to halothane (250 ± 27 nM; $P < 0.0001$) compared to the untreated *RYR1*-p.R163C/dominant-negative TRPC6 left leg muscle (fig. 8B).

Measurements of TRPC3 and TRPC6 Expression in Muscle Cells

We determined the expression of TRPC3 and TRPC6 channels in gastrocnemius muscle homogenates from wild-type, wild-type/dominant-negative TRPC6, *RYR1*-p.R163C, and *RYR1*-p.R163C/dominant-negative TRPC6 mice. As expected from our previous studies on murine models relevant to MH,[14] Western blot analysis demonstrated a statistically significantly increased expression of both TRPC3 and TRPC6 proteins in *RYR1*-p.R163C compared to wild-type muscles ($P < 0.0001$ and $P < 0.0001$, respectively). Furthermore, as expected, we were able to see a statistically significant increase in TRPC6 expression in wild-type/dominant-negative TRPC6 and *RYR1*-p.R163C/dominant-negative TRPC6 muscles compared to controls ($P = 0.002$ and $P = 0.008$, respectively). Unexpectedly, we observed that concomitantly with the expected transgenic overexpression of TRPC6, there was a statistically significant increase in the expression of TRPC3 protein in both wild-type/dominant-negative TRPC6 ($P = 0.013$) compared to wild-type ($P = 0.002$) and *RYR1*-p.R163C/dominant-negative TRPC6 compared to *RYR1*-p.R163C muscles ($P = 0.014$). Figure 9A shows a representative Western blot from the four genotypes and quantification graphs reflecting relative expression levels of TRPC3 and TRPC6 proteins normalized to the expression of glyceraldehyde-3-phosphate dehydrogenase (fig. 9B).

Discussion

We have demonstrated that muscle-specific overexpression of the nonconducting TRPC6 channel both reduced intracellular Ca^{2+} concentration in *RYR1*-p.R163C animals at rest and reduced the absolute maximum levels of intracellular Ca^{2+} concentration reached during exposure to halothane. Despite this, its expression did not restore intracellular Ca^{2+} concentration to wild-type levels, and although its expression increased the length of survival after the exposure to halothane, it was unable to rescue the lethal phenotype. The physiologic effect of muscle-specific expression of a dominant-negative TRPC6 on TRPC6 function was confirmed by the marked attenuation of reactivity of expressing muscle fibers to the TRPC6 activator hyperforin. Although there was a compensatory increase in expression of TRPC3 in dominant-negative

TRPC6 mice, this does not explain the failure of molecular inhibition of TRPC6 channels to fully restore responses in *RYR1*-p. R163C animals and fibers to that of wild type because the addition of ethyl-1-(4-(2,3,3-trichloroacrylamide) phenyl)-5-(trifluoromethyl)-1H-pyrazole-4-carboxylate, a TRPC3 blocker, still resulted in elevated intracellular Ca^{2+} concentrations at rest and during exposure to halothane. Indeed, the contribution of TRPC3 to intracellular Ca^{2+} concentration was proportionally similar in *RYR1*-p. R163C fibers in the presence or absence of dominant-negative TRPC6. Our findings of an effect of dominant-negative TRPC6 and ethyl-1-(4-(2,3,3-trichloroacrylamide) phenyl)-5-(trifluoromethyl)-1H-pyrazole-4-carboxylate in wild-type fibers demonstrate that TRPC3/6 channels contribute to physiologic levels of intracellular Ca^{2+} concentration in skeletal muscle. It is possible that their role is to help maintain intracellular Ca^{2+} store content during muscle activity, and this effect could be mediated through diacylglycerol signaling in response to elevations in intracellular Ca^{2+} concentration.

Molecular genetic studies have established the *RYR1* gene encoding the skeletal muscle sarcoplasmic reticulum Ca^{2+} release channel as the primary locus for MH susceptibility,[2,4,5] and secondary loci have been identified in other proteins involved with RyR1 in excitation–contraction coupling[26,27] that are thought to sensitize the RyR1 channel. A common characteristic of muscle expressing MH-RyR1 variants is an increased intracellular Ca^{2+} concentration that is thought to be caused by increased RyR1 leak.[8,9,11,19,28,29] However, evidence accumulated over the past decade suggests more complex molecular mechanisms by which a sensitized RyR1 channel results in a MH reaction upon exposure to triggering anesthetics, as well as nonanesthetic phenotypes associated with MH susceptibility.

The importance of extracellular Ca^{2+} to the effects of halothane in MH-susceptible muscle was suggested more than 40 yr ago.[30] More recently, Duke *et al.*,[31] Eltit *et al.*,[13] and Lopez *et al.*[14] have demonstrated transsarcolemmal Ca^{2+} influx in human and mouse MH muscle, which appears to be mediated by store-operated Ca^{2+} entry, canonical transient receptor potential channels, or both. The current study both confirms augmented expression of TRPC3 and TRPC6 in MH muscle fibers[13,14] and unequivocally demonstrates, through specific molecular inhibition, the contribution of TRPC channels that is predominantly mediated through TRPC6. Indeed, the intracellular Ca^{2+} dyshomeostasis observed in MH-susceptible muscle could not be sustained solely by sarcoplasmic reticulum Ca^{2+} leak/release, but instead, a combination of this and TRPC-mediated transsarcolemmal Ca^{2+} influx were required, with the latter being the major player in terms of Ca^{2+} contribution.

TRPC channels constitute a large and functionally versatile superfamily of cation channel proteins expressed in many cell types that control influxes of Ca^{2+} and other cations (sodium, lithium, and magnesium)[32] to regulate diverse cellular processes. In skeletal muscle, they seem to be involved in muscle development, store-operated entry of Ca^{2+}, response to stretch,[33] and modulation of glucose transport.[34] TRPC channels are activated by diacylglycerol generated in response to phospholipase C–induced phosphatidylinositol 4,5-bisphosphate hydrolysis.[22] A driving force behind the recent research in the field of TRPCs in muscle is the idea that TRPCs could be involved through abnormal Ca^{2+} signaling

in several striated muscle pathologies, such as Duchenne muscular dystrophy,[33,35,36] myocardial remodeling and hypertrophy,[34] and MH.[13,14]

Defining the large but still partial contributions of TRPC3 and TRPC6 to elevated intracellular Ca^{2+} concentration in MH-susceptible muscle at rest and during a MH episode draws attention to other contributing mechanisms. It is possible that sarcoplasmic reticulum Ca^{2+} leak could fully explain residual increases in intracellular Ca^{2+} concentration, but it is the responses to halothane we find especially intriguing. We have previously reported that the reverse mode function of the sodium–calcium exchanger contributes to the elevation of intracellular Ca^{2+} during the MH episode,[18] and this may also explain the findings in the muscle of *RYR1*-p.R163C/dominant-negative TRPC6 mice pretreated with the TRPC3 inhibitor ethyl-1-(4-(2,3,3-trichloroacrylamide)phenyl)-5-(trifluoromethyl)-1H-pyrazole-4-carboxylate before addition of halothane. The reverse-mode sodium–calcium exchanger can be activated after localized intracellular sodium accumulation through nonselective TRPC[13,14] and store-operated calcium channels. Furthermore, the sodium–calcium exchanger has also been demonstrated to interact both physically and functionally with certain TRPC channels, and evidence has been presented for the link between stromal interaction molecule 1–mediated sodium influx and the activation of the sodium–calcium exchanger.[37] Here there was an initial, relatively small increase in intracellular Ca^{2+} concentration to a level that was sustained for approximately 10 min before the beginning of a second, slower, more marked and progressive increase that paralleled the increase in the rectal temperature of the animal. Such a pattern suggests that the initial plateau represents a new equilibrium in which increased calcium sequestration compensates for increased sarcoplasmic reticulum calcium release. Clearly this status quo cannot be sustained. Decompensation might occur if there is disruption of ATP production, which could occur with excessive mitochondrial uptake of calcium, leading to reduced calcium sequestration capacity. Alternatively, mitochondrial dysfunction secondary to calcium uptake could result in increased production of reactive oxygen species that can result in increased RyR1-mediated calcium release.[38,39] A further possibility is that the sarcoplasmic reticulum calcium content decreases during the plateau phase to reach the level at which store-operated calcium entry is initiated, leading to a massive sustained influx of extracellular calcium.[31]

This study is not without limitations. The main limitation of this work is that it is conducted using mice and mouse tissue rather than humans and human tissue. Although murine models relevant to MH appear more sensitive to environmental heat stress than MH-susceptible patients, they recapitulate the human condition in many other respects, including increased intracellular Ca^{2+} concentration,[9,28,40] dependence on extracellular calcium,[31] and mitochondrial dysfunction.[41] We have also not demonstrated that skeletal muscle–specific expression of a nonconducting dominant-negative TRPC6 completely abolishes TRPC6 conductance, although previous work with this construct suggests this is likely.[15] Finally, although we have used molecular inhibition of TRPC6, our conclusions concerning the effect of ethyl-1-(4-(2,3,3-trichloroacrylamide)phenyl)-5-(trifluoromethyl)-1H-pyrazole-4-carboxylate on TRPC3 must be more guarded because selectivity of pharmacologic reagents can never be guaranteed.

In summary, these results demonstrate that nonselective sarcolemmal cation permeability mediated by TRPC6 and TRPC3 plays a critical role in causing cytosolic Ca^{2+} overload both at rest and during a MH crisis. This improved understanding of the underlying mechanisms of MH may assist in the design of new therapies and the identification of more selective pharmacologic agents other than our current accepted standard, dantrolene, to prevent or reverse the MH episodes.

Supplementary Material

Refer to Web version on PubMed Central for supplementary material.

Acknowledgments

The authors are grateful to Jeffery D. Molkentin, Ph.D., Howard Hughes Medical Institute, Molecular Cardiovascular Biology, Cincinnati Children's Hospital Medical Center, Cincinnati, Ohio, for generously providing us with the transgenic mice with skeletal muscle–specific overexpression of a nonconducting TRPC6 channel; and Shane Antrobus, B.S., Department of Molecular Biosciences, School of Veterinary Medicine, University of California at Davis, Davis, California, for his valuable technical assistance.

Research Support

Supported by grant Nos. 1R01AR068897 and P01AR-05235 from the National Institute of Arthritis, Musculoskeletal and Skin Diseases, National Institutes of Health (Bethesda, Maryland; to Drs. Allen, Hopkins, and Lopez), grant No. 21543 from the French Muscular Dystrophy Association (AFM; Evry, France; to Dr. Lopez), and funds from the Florida Heart Foundation (Miami, Florida; to Drs. Lopez, Uryash, and Adams).

References

1. Rosenberg H, Pollock N, Schiemann A, Bulger T, Stowell K: Malignant hyperthermia: A review. Orphanet J Rare Dis 2015; 10:93 [PubMed: 26238698]
2. MacLennan DH, Duff C, Zorzato F, Fujii J, Phillips M, Korneluk RG, Frodis W, Britt BA, Worton RG: Ryanodine receptor gene is a candidate for predisposition to malignant hyperthermia. Nature 1990; 343:559–61 [PubMed: 1967823]
3. Kausch K, Lehmann-Horn F, Janka M, Wieringa B, Grimm T, Müller CR: Evidence for linkage of the central core disease locus to the proximal long arm of human chromosome 19. Genomics 1991; 10:765–9 [PubMed: 1889818]
4. Robinson R, Carpenter D, Shaw MA, Halsall J, Hopkins P: Mutations in RYR1 in malignant hyperthermia and central core disease. Hum Mutat 2006; 27:977–89 [PubMed: 16917943]
5. Jurkat-Rott K, McCarthy T, Lehmann-Horn F: Genetics and pathogenesis of malignant hyperthermia. Muscle Nerve 2000; 23:4–17 [PubMed: 10590402]
6. Miller DM, Daly C, Aboelsaod EM, Gardner L, Hobson SJ, Riasat K, Shepherd S, Robinson RL, Bilmen JG, Gupta PK, Shaw MA, Hopkins PM: Genetic epidemiology of malignant hyperthermia in the UK. Br J Anaesth 2018; 121:944–52 [PubMed: 30236257]
7. López JR, Alamo L, Caputo C, Wikinski J, Ledezma D: Intracellular ionized calcium concentration in muscles from humans with malignant hyperthermia. Muscle Nerve 1985; 8:355–8 [PubMed: 16758579]
8. López JR, Alamo LA, Jones DE, Papp L, Allen PD, Gergely J, Sréter FA: $[Ca^{2+}]_i$ in muscles of malignant hyperthermia susceptible pigs determined *in vivo* with Ca^{2+} selective microelectrodes. Muscle Nerve 1986; 9:85–6 [PubMed: 3951486]
9. Yang T, Esteve E, Pessah IN, Molinski TF, Allen PD, Lopez JR: Elevated resting $[Ca^{2+}]_i$ in myotubes expressing malignant hyperthermia RyR1 cDNAs is partially restored by modulation of passive calcium leak from the SR. Am J Physiol Cell Physiol 2007; 292:C1591–8 [PubMed: 17182726]

10. Eltit JM, Bannister RA, Moua O, Altamirano F, Hopkins PM, Pessah IN, Molinski TF, López JR, Beam KG, Allen PD: Malignant hyperthermia susceptibility arising from altered resting coupling between the skeletal muscle L-type Ca^{2+} channel and the type 1 ryanodine receptor. Proc Natl Acad Sci USA 2012; 109:7923–8 [PubMed: 22547813]
11. López JR, Allen PD, Alamo L, Jones D, Sreter FA: Myoplasmic free [Ca^{2+}] during a malignant hyperthermia episode in swine. Muscle Nerve 1988; 11:82–8 [PubMed: 3340102]
12. Yuen B, Boncompagni S, Feng W, Yang T, Lopez JR, Matthaei KI, Goth SR, Protasi F, Franzini-Armstrong C, Allen PD, Pessah IN: Mice expressing T4826I-RYR1 are viable but exhibit sex- and genotype-dependent susceptibility to malignant hyperthermia and muscle damage. FASEB J 2012; 26:1311–22 [PubMed: 22131268]
13. Eltit JM, Ding X, Pessah IN, Allen PD, Lopez JR: Nonspecific sarcolemmal cation channels are critical for the pathogenesis of malignant hyperthermia. FASEB J 2013; 27:991–1000 [PubMed: 23159934]
14. Lopez JR, Kaura V, Hopkins P, Liu X, Uryach A, Adams J, Allen PD: Transient receptor potential cation channels and calcium dyshomeostasis in a mouse model relevant to malignant hyperthermia. Anesthesiology 2020; 133:364–76 [PubMed: 32665491]
15. Millay DP, Goonasekera SA, Sargent MA, Maillet M, Aronow BJ, Molkentin JD: Calcium influx is sufficient to induce muscular dystrophy through a TRPC-dependent mechanism. Proc Natl Acad Sci USA 2009; 106:19023–8 [PubMed: 19864620]
16. Hofmann T, Schaefer M, Schultz G, Gudermann T: Subunit composition of mammalian transient receptor potential channels in living cells. Proc Natl Acad Sci USA 2002; 99:7461–6 [PubMed: 12032305]
17. Tang Q, Guo W, Zheng L, Wu JX, Liu M, Zhou X, Zhang X, Chen L: Structure of the receptor-activated human TRPC6 and TRPC3 ion channels. Cell Res 2018; 28:746–55 [PubMed: 29700422]
18. Altamirano F, Eltit JM, Robin G, Linares N, Ding X, Pessah IN, Allen PD, López JR: Ca^{2+} influx via the Na^{+}/Ca^{2+} exchanger is enhanced in malignant hyperthermia skeletal muscle. J Biol Chem 2014; 289:19180–90 [PubMed: 24847052]
19. López JR, Alamo L, Caputo C, DiPolo R, Vergara S: Determination of ionic calcium in frog skeletal muscle fibers. Biophys J 1983; 43:1–4 [PubMed: 6603872]
20. Altamirano F, Perez CF, Liu M, Widrick J, Barton ER, Allen PD, Adams JA, Lopez JR: Whole body periodic acceleration is an effective therapy to ameliorate muscular dystrophy in mdx mice. PLoS One 2014; 9:e106590 [PubMed: 25181488]
21. Laemmli UK: Cleavage of structural proteins during the assembly of the head of bacteriophage T4. Nature 1970; 227:680–5 [PubMed: 5432063]
22. Hofmann T, Obukhov AG, Schaefer M, Harteneck C, Gudermann T, Schultz G: Direct activation of human TRPC6 and TRPC3 channels by diacylglycerol. Nature 1999; 397:259–63 [PubMed: 9930701]
23. Aires V, Hichami A, Boulay G, Khan NA: Activation of TRPC6 calcium channels by diacylglycerol (DAG)–containing arachidonic acid: A comparative study with DAG-containing docosahexaenoic acid. Biochimie 2007; 89:926–37 [PubMed: 17532549]
24. Leuner K, Kazanski V, Müller M, Essin K, Henke B, Gollasch M, Harteneck C, Müller WE: Hyperforin: A key constituent of St. John's wort specifically activates TRPC6 channels. FASEB J 2007; 21:4101–11 [PubMed: 17666455]
25. Kiyonaka S, Kato K, Nishida M, Mio K, Numaga T, Sawaguchi Y, Yoshida T, Wakamori M, Mori E, Numata T, Ishii M, Takemoto H, Ojida A, Watanabe K, Uemura A, Kurose H, Morii T, Kobayashi T, Sato Y, Sato C, Hamachi I, Mori Y: Selective and direct inhibition of TRPC3 channels underlies biological activities of a pyrazole compound. Proc Natl Acad Sci USA 2009; 106:5400–5 [PubMed: 19289841]
26. Robinson RL, Monnier N, Wolz W, Jung M, Reis A, Nuernberg G, Curran JL, Monsieurs K, Stieglitz P, Heytens L, Fricker R, van Broeckhoven C, Deufel T, Hopkins PM, Lunardi J, Mueller CR: A genome wide search for susceptibility loci in three European malignant hyperthermia pedigrees. Hum Mol Genet 1997; 6:953–61 [PubMed: 9175745]

27. Stamm DS, Powell CM, Stajich JM, Zismann VL, Stephan DA, Chesnut B, Aylsworth AS, Kahler SG, Deak KL, Gilbert JR, Speer MC: Novel congenital myopathy locus identified in Native American Indians at 12q13.13–14.1. Neurology 2008; 71:1764–9 [PubMed: 18843099]
28. Yang T, Riehl J, Esteve E, Matthaei KI, Goth S, Allen PD, Pessah IN, Lopez JR: Pharmacologic and functional characterization of malignant hyperthermia in the R163C RyR1 knock-in mouse. Anesthesiology 2006; 105:1164–75 [PubMed: 17122579]
29. Lopez JR, Kaura V, Diggle CP, Hopkins PM, Allen PD: Malignant hyperthermia, environmental heat stress, and intracellular calcium dysregulation in a mouse model expressing the p.G2435R variant of RYR1. Br J Anaesth 2018; 121:953–61 [PubMed: 30236258]
30. Nelson TE, Bedell DM, Jones EW: Porcine malignant hyperthermia: Effects of temperature and extracellular calcium concentration on halothane-induced contracture of susceptible skeletal muscle. Anesthesiology 1975; 42:301–6 [PubMed: 1115384]
31. Duke AM, Hopkins PM, Calaghan SC, Halsall JP, Steele DS: Store-operated Ca^{2+} entry in malignant hyperthermia-susceptible human skeletal muscle. J Biol Chem 2010; 285:25645–53 [PubMed: 20566647]
32. Owsianik G, Talavera K, Voets T, Nilius B: Permeation and selectivity of TRP channels. Annu Rev Physiol 2006; 68:685–717 [PubMed: 16460288]
33. Lopez JR, Uryash A, Faury G, Estève E, Adams JA: Contribution of TRPC channels to intracellular Ca^{2+} dyshomeostasis in smooth muscle from mdx mice. Front Physiol 2020; 11:126 [PubMed: 32153426]
34. Eder P: Cardiac remodeling and disease: SOCE and TRPC signaling in cardiac pathology. Adv Exp Med Biol 2017; 993:505–21 [PubMed: 28900930]
35. Mijares A, Altamirano F, Kolster J, Adams JA, López JR: Age-dependent changes in diastolic Ca^{2+} and Na^{+} concentrations in dystrophic cardiomyopathy: Role of Ca^{2+} entry and IP3. Biochem Biophys Res Commun 2014; 452:1054–9 [PubMed: 25242522]
36. Matsumura CY, Taniguti AP, Pertille A, Santo Neto H, Marques MJ: Stretch-activated calcium channel protein TRPC1 is correlated with the different degrees of the dystrophic phenotype in mdx mice. Am J Physiol Cell Physiol 2011; 301:C1344–50 [PubMed: 21900691]
37. Liu B, Peel SE, Fox J, Hall IP: Reverse mode Na^{+}/Ca^{2+} exchange mediated by STIM1 contributes to Ca^{2+} influx in airway smooth muscle following agonist stimulation. Respir Res 2010; 11:168 [PubMed: 21126331]
38. Dridi H, Yehya M, Barsotti R, Reiken S, Angebault C, Jung B, Jaber S, Marks AR, Lacampagne A, Matecki S: Mitochondrial oxidative stress induces leaky ryanodine receptor during mechanical ventilation. Free Radic Biol Med 2020; 146:383–91 [PubMed: 31756525]
39. Lotteau S, Ivarsson N, Yang Z, Restagno D, Colyer J, Hopkins P, Weightman A, Himori K, Yamada T, Bruton J, Steele D, Westerblad H, Calaghan S: A mechanism for statin-induced susceptibility to myopathy. JACC Basic Transl Sci 2019; 4:509–23 [PubMed: 31468006]
40. Yang T, Allen PD, Pessah IN, Lopez JR: Enhanced excitation-coupled calcium entry in myotubes is associated with expression of RyR1 malignant hyperthermia mutations. J Biol Chem 2007; 282:37471–8 [PubMed: 17942409]
41. Chang L, Daly C, Miller DM, Allen PD, Boyle JP, Hopkins PM, Shaw MA: Permeabilised skeletal muscle reveals mitochondrial deficiency in malignant hyperthermia-susceptible individuals. Br J Anaesth 2019; 122:613–21 [PubMed: 30916033]

EDITOR'S PERSPECTIVE

What We Already Know about This Topic

- The type 1 ryanodine receptor (*RYR1*) gene encoding the skeletal muscle sarcoplasmic reticulum Ca^{2+} release channel is the primary locus for malignant hyperthermia susceptibility
- Secondary loci have been identified in other proteins involved with RyR1 in excitation–contraction coupling that are thought to sensitize the RyR1 channel
- Transient receptor potential canonical channels constitute a large and functionally versatile superfamily of cation channel proteins expressed in many cell types that control influxes of Ca^{2+} and other cations to regulate diverse cellular processes

What This Article Tells Us That Is New

- Muscle-specific overexpression of the nonconducting transient receptor potential canonical 6 channel both reduced intracellular Ca^{2+} concentration in RYR1-p.R163C mice at rest and reduced the absolute maximum levels of intracellular Ca^{2+} concentration reached during exposure to halothane
- Despite this, its overexpression did not restore intracellular Ca^{2+} concentration to wild-type levels, and although its overexpression increased the length of survival after halothane exposure, it was unable to rescue the lethal phenotype

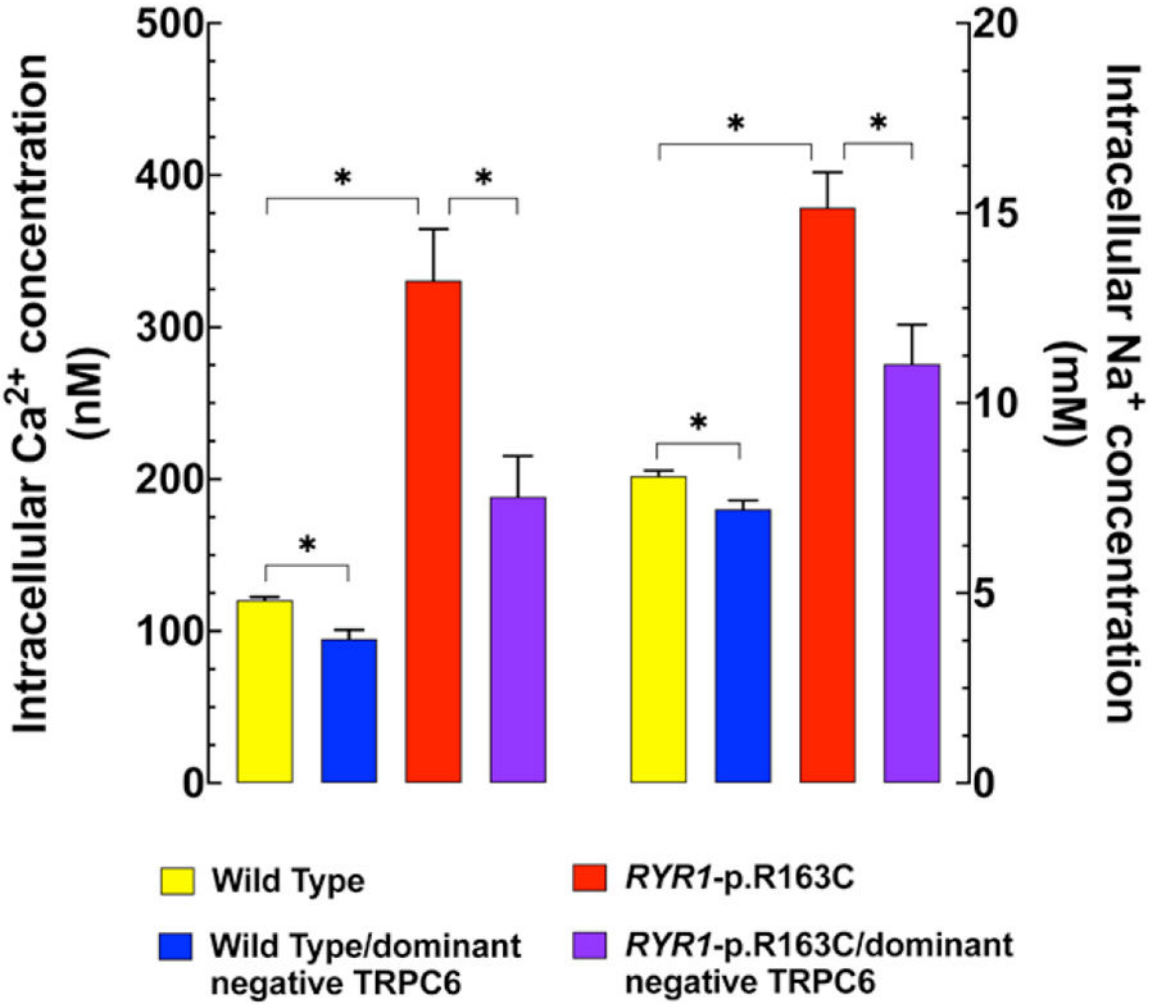

Fig. 1.

Reduced intracellular Ca^{2+} and sodium (Na^{+}) concentrations in muscle fibers expressing a dominant-negative transient receptor potential canonical 6 (TRPC6) channel. Intracellular Ca^{2+} or sodium concentration was measured on the superficial vastus lateralis muscle fibers *in vivo* in wild-type, wild-type/dominant-negative TRPC6, *RYR1*-p.R163C, and *RYR1*-p.R163C/dominant-negative TRPC6 mice using double-barreled ion-specific microelectrodes. Seven mice per genotype; wild-type, 35 cells; wild-type dominant-negative TRPC6, 34 cells; *RYR1*-p. R163C, 25 cells; *RYR1*-p.R163C/dominant 35 cells for intracellular Ca^{2+} concentration measurements. For intracellular sodium concentration measurements, 4 mice per genotype wild type, 20 cells; wild-type dominant-negative TRPC6, 15 cells; *RYR1*-p. R163C, 15 cells; *RYR1*-p.R163C/dominant-negative TRPC6, 15 cells. The values are expressed as means ± SD for each condition. Statistical analysis was done using a one-way ANOVA with Tukey's posttest. $*P \leq 0.05$.

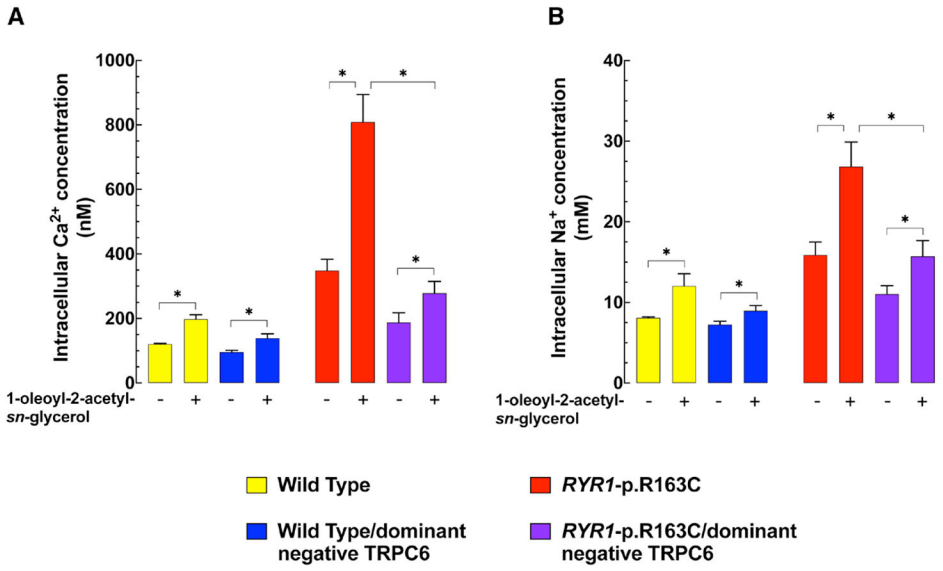

Fig. 2.

Expressing a dominant-negative transient receptor potential canonical 6 (TRPC6) channel reduces the elevation of intracellular Ca^{2+} and sodium (Na^{+}) concentrations elicited by 1-oleoyl-2-acetyl-*sn*-glycerol. Exposure of quiescent flexor digitorum brevis muscle fibers isolated from wild-type, wild-type/dominant-negative TRPC6, *RYR1*-p.R163C, and *RYR1*-p.R163C/dominant-negative TRPC6 mice to 100 μM 1-oleoyl-2-acetyl-*sn*-glycerol induced an elevation of intracellular Ca^{2+} (*A*) and sodium concentration (*B*). Expression of dominant-negative TRPC6 reduced the effect of 1-oleoyl-2-acetyl-*sn*-glycerol on both intracellular Ca^{2+} (*A*) and sodium (*B*) concentrations in both wild-type and *RYR1*-p.R163C muscle fibers. The experimental conditions are indicated on the *horizontal axes*. For intracellular Ca^{2+} concentration measurements: 5 mice per genotype, wild-type, 25 cells; wild-type dominant-negative TRPC6, 20 cells; *RYR1*-p.R163C 20 cells; *RYR1*-p.R163C/dominant-negative, n = 21 for intracellular Ca^{2+} concentration measurements. For intracellular sodium concentration measurements: 3 mice per genotype. Wild-type, 15 cells; wild-type dominant-negative TRPC6, 17 cells; *RYR1*-p.R163C, 18 cells; *RYR1*-p.R163C/dominant-negative TRPC6, 15 cells. The values are expressed as means ± SD for each condition. Statistical analysis was done using a one-way ANOVA with Tukey's posttest. **P* ≤ 0.05.

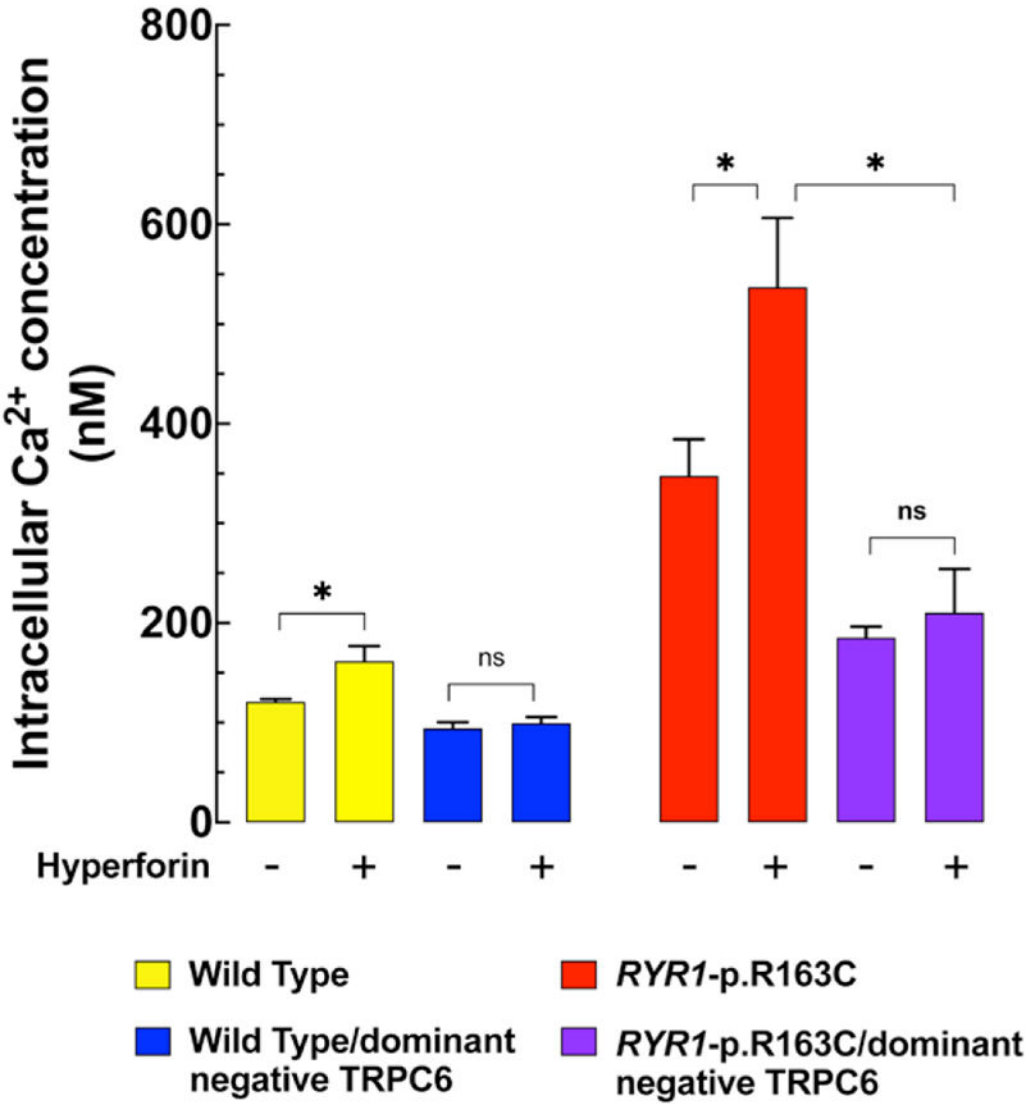

Fig. 3.

Hyperforin induced an elevation of intracellular Ca^{2+} concentration. Incubation of flexor digitorum brevis muscle fibers isolated from wild-type, wild-type/dominant-negative transient receptor potential canonical 6 (TRPC6), *RYR1*-p.R163C, and *RYR1*-p.R163C/dominant-negative TRPC6 mice with 10 μM hyperforin produced a statistically significant ($P < 0.0001$) increase in intracellular Ca^{2+} concentration in all genotypes, but the effect was more marked in *RYR1*-p.R163C fibers than in wild type. Expression of dominant-negative TRPC6 in wild type and *RYR1*-p.R163C reduced the effect of hyperforin. The experimental conditions used are indicated on the *horizontal axis.* For intracellular Ca^{2+} concentration measurements: Five mice per genotype, wild-type, 19 cells; wild-type dominant-negative TRPC6, 20 cells; *RYR1*-p.R163C, 22 cells; *RYR1*-p.R163C/dominant-negative, TRPC6 20 cells. The values are expressed as means ± SD for each condition. Statistical analysis was done using a one-way ANOVA with Tukey's posttest. *$P \leq 0.05$.

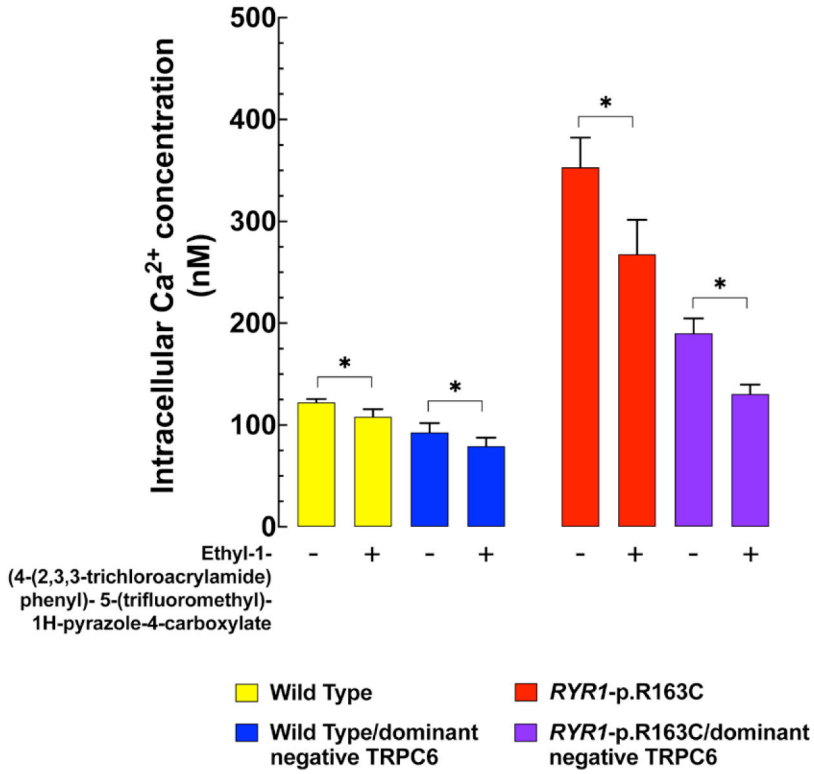

Fig. 4.

Effect of ethyl-1-(4-(2,3,3-trichloroacrylamide)phenyl)-5-(trifluoromethyl)-1H-pyrazole-4-carboxylate on intracellular Ca^{2+} and sodium. Ethyl-1-(4-(2,3,3-trichloro-acrylamide)phenyl)-5-(trifluoromethyl)-1H-pyrazole-4-carboxylate (10 μM) reduced intracellular Ca^{2+} concentration in the flexor digitorum brevis muscles of all genotypes. The experimental conditions used are indicated on the *horizontal axis.* For intracellular Ca^{2+} determinations: 5 mice per genotype, wild-type, 20 cells; wild-type–ethyl-1-(4-(2,3,3-trichloro-acrylamide) phenyl)-5-(trifluoromethyl)-1H-pyrazole-4-carboxylate, 23 cells; wild-type dominant-negative transient receptor potential canonical 6 (TRPC6), 19 cells; wild-type dominant-negative TRPC6–ethyl-1-(4-(2,3,3-trichloro-acrylamide)phenyl)-5-(trifluoromethyl)-1H-pyrazole-4-carboxylate, 21 cells; *RYR1*-p.R163C, 22 cells; *RYR1*-p.R163C–ethyl-1-(4-(2,3,3-trichloro-acrylamide)phenyl)-5-(trifluoromethyl)-1H-pyrazole-4-carboxylate, 21 cells; *RYR1*-p.R163C dominant-negative TRPC6, 20 cells; *RYR1*-p.R163C dominant-negative TRPC6–ethyl-1-(4-(2,3,3-trichloro-acrylamide)phenyl)-5-(trifluoromethyl)-1H-pyrazole-4-carboxylate, 22 cells. The values are expressed as means ± SD for each condition. Statistical analysis was done using a one-way ANOVA with Tukey's posttest. $*P \leq 0.05$.

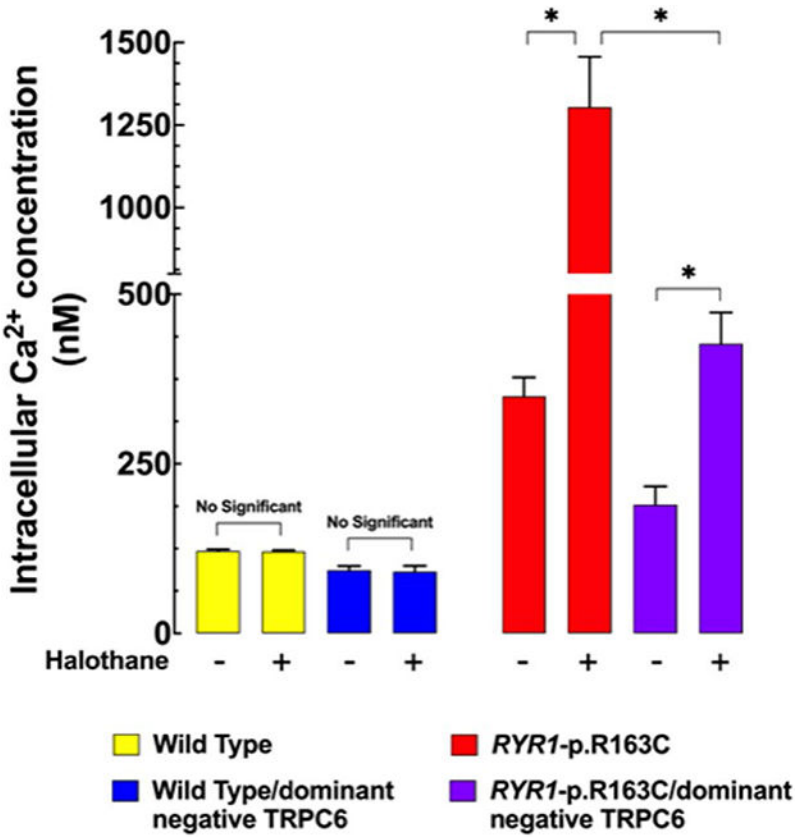

Fig. 5.

Expression of dominant-negative transient receptor potential canonical 6 (TRPC6) reduced the increase of intracellular Ca^{2+} concentration in RYR1-p.R163C muscle during exposure to halothane. Intracellular Ca^{2+} concentration was measured *in vivo* in the vastus lateralis fibers of wild-type, wild-type/dominant-negative TRPC6, *RYR1*-p.R163C, and *RYR1*-p.R163C dominant/negative TRPC6 before and after the inhalation of 2% halothane. In wild-type muscle fibers, halothane did not provoke elevation in intracellular Ca^{2+} concentration, whereas in *RYR1*-p.R163C, it induced a robust and immediate elevation of intracellular Ca^{2+} concentration. Expression of dominant-negative TRPC6 in *RYR1*-p.R163C muscle reduced intracellular Ca^{2+} concentration and statistically significantly attenuated the increase in intracellular Ca^{2+} concentration during inhalation of halothane. The experimental conditions used are indicated on the *horizontal axis.* For intracellular Ca^{2+} concentration measurements in 7 mice per genotype, wild-type, 35 cells; wild-type dominant-negative TRPC6, 32 cells; *RYR1*-p.R163C, 23 cells; *RYR1*-p.R163C/dominant-negative TRPC6, 37 cells. The values are expressed as means ± SD for each condition. Statistical analysis was done using a one-way ANOVA with Tukey's posttest. $*P \leq 0.05$.

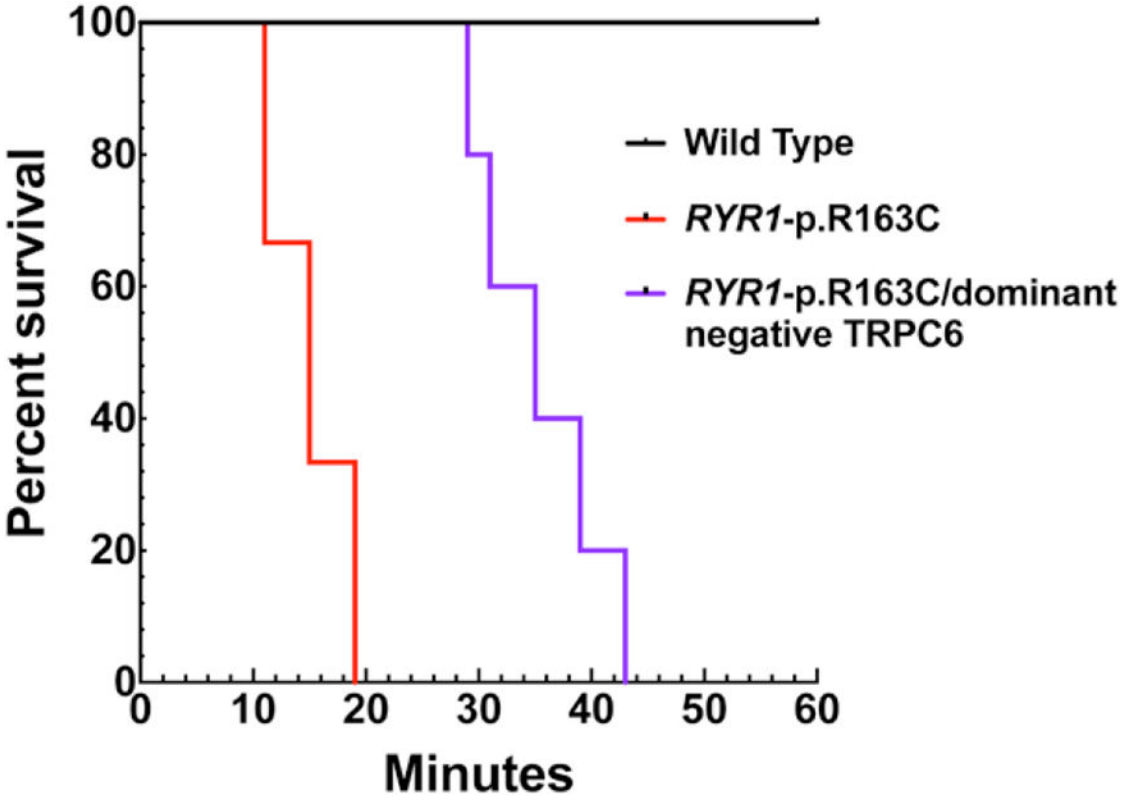

Fig. 6.

The survival of R163C mice is enhanced by expression. Kaplan–Meier survival curves reveal that expression of dominant transient receptor potential canonical 6 (TRPC6) statistically significantly increased the mice survival time in *RYR1*-p.R163C mice from 15.3 ± 3 min to 35.5 ± 5 min *RYR1*-p.R163C/dominant-negative TRPC6. Seven mice per genotype. The values are expressed as means ± SD for each condition. Statistical analysis was done using a Mantel–Cox log rank test. $*P \leq 0.05$.

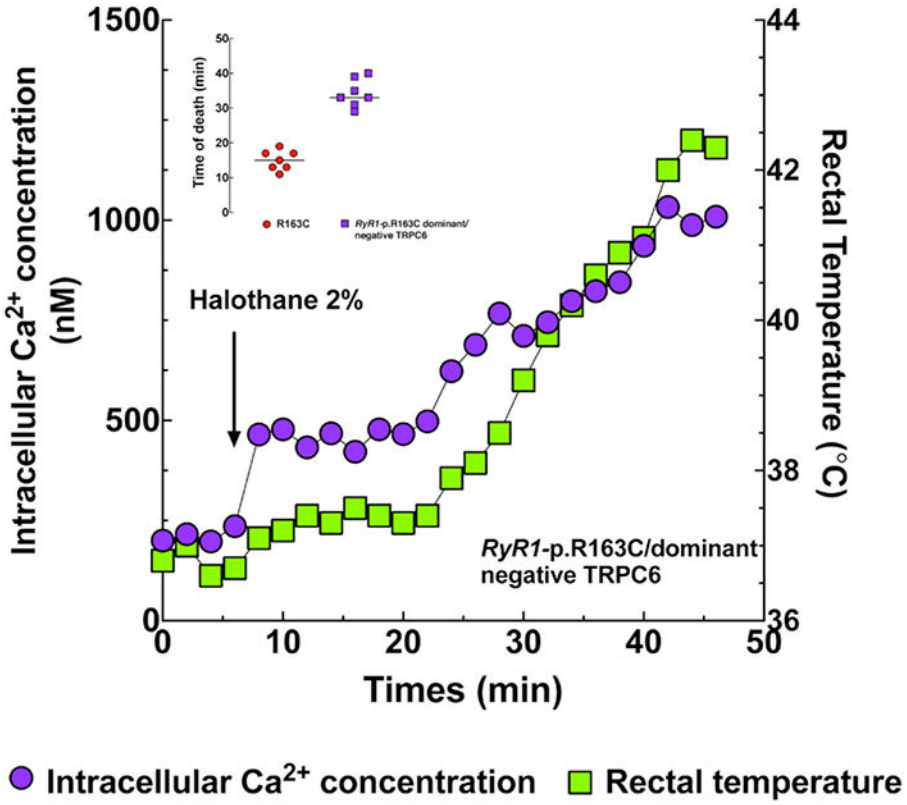

Fig. 7.

Time course of changes in intracellular Ca^{2+} and rectal temperature in a mouse expressing dominant-negative transient receptor potential canonical 6 (TRPC6). A typical experiment was carried out *in vivo* in an anesthetized (ketamine/xylazine) *RYR1*-p.R163C/dominant-negative TRPC6 mouse. Intracellular calcium concentrations on the superficial fibers of the vastus lateralis muscle and rectal temperature were measured simultaneously before and after halothane 2% inhalation. The *inset* in the *upper left corner* shows the time of death after halothane inhalation.

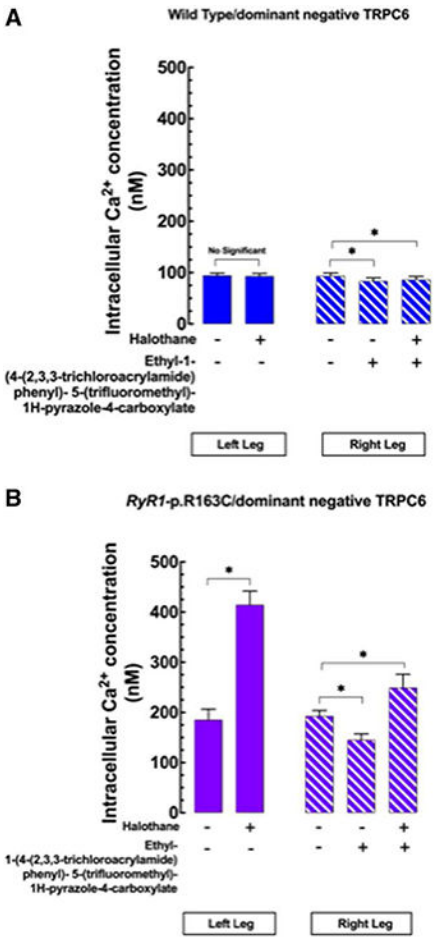

Fig. 8.

Ethyl-1-(4-(2,3,3-trichloroacrylamide)phenyl)-5-(trifluoromethyl)-1H-pyrazole-4-carboxylate reduces intracellular Ca^{2+} concentration in RYR1-p.R163C/dominant-negative transient receptor potential canonical 6 (TRPC6) skeletal muscle cells. Intracellular Ca^{2+} concentration was measured in both the right and left vastus lateralis muscle of wild-type/dominant-negative TRPC6 (*A*) and *RYR1*-p.R163C/dominant-negative TRPC6 muscles (*B*). In both, the right leg was superfused with the TRPC3 blocker ethyl-1-(4-(2,3,3-trichloroacrylamide)phenyl)-5-(trifluoromethyl)-1H-pyrazole-4-carboxylate, and Ca^{2+} was measured a second time, after which the animal was exposed to 2% halothane, and intracellular Ca^{2+} concentration was measured in both the right and left vastus lateralis muscles a final time. Five mice per genotype, wild-type dominant-negative TRPC6 (left leg), 20 cells; wild-type dominant-negative TRPC6 (left leg)–halothane, 18 cells; wild-type dominant-negative TRPC6 (right leg), 17 cells; wild-type dominant-negative TRPC6 (right leg)–ethyl-1-(4-(2,3,3-trichloroacrylamide)phenyl)-5-(trifluoromethyl)-1H-pyrazole-4-carboxylate, 20 cells; wild-type dominant-negative TRPC6 (right leg)–ethyl-1-(4-(2,3,3-trichloroacrylamide)phenyl)-5-(trifluoromethyl)-1H-pyrazole-4-carboxylate and halothane, 19 cells. *RYR1*-p.R163C/dominant-negative TRPC6 (left leg), n = 22; *RYR1*-p.R163C/dominant-negative TRPC6 (left leg)–halothane, 22 cells; *RYR1*-p.R163C/dominant-negative TRPC6 (right leg), 21 cells; *RYR1*-p.R163C/dominant-negative

TRPC6 (right leg)–ethyl-1-(4-(2,3,3-trichloroacrylamide)phenyl)-5-(trifluoromethyl)-1H-pyrazole-4-carboxylate and halothane, 21 cells; *RYR1*-p.R163C/dominant-negative TRPC6 (right leg)–ethyl-1-(4-(2,3,3-trichloroacrylamide)phenyl)-5-(trifluoromethyl)-1H-pyrazole-4-carboxylate and halothane, 22 cells. The experimental conditions used are indicated on the *horizontal axes.* The values are expressed as means ± SD for each condition. Statistical analysis was done using a one-way ANOVA with Tukey's posttest. $*P \leq 0.05$.

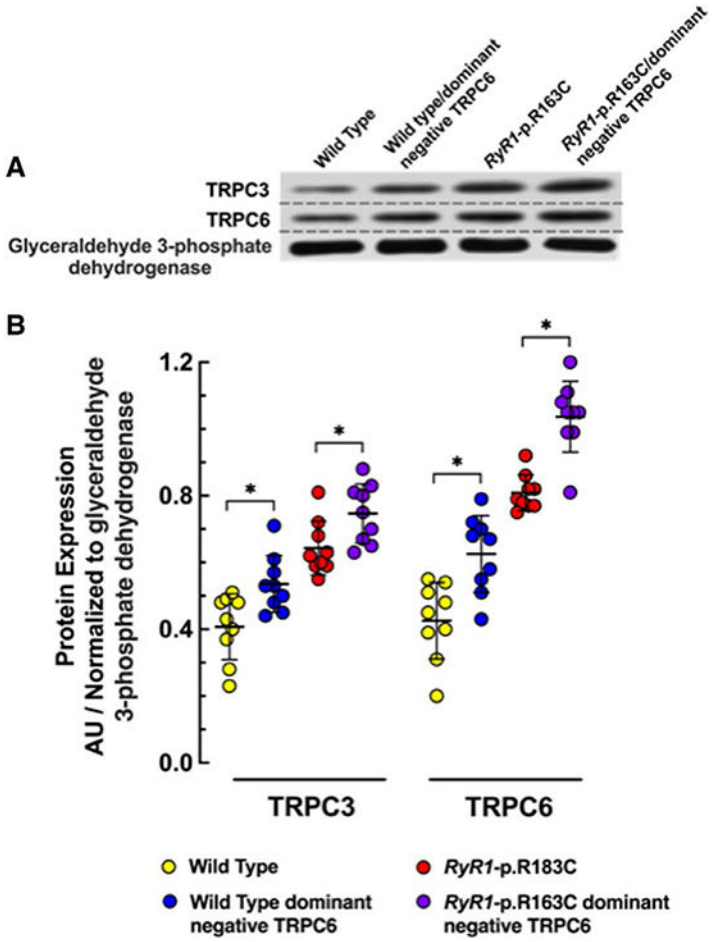

Fig. 9.

Measurements of transient receptor potential canonical (TRPC) 3 and TRPC6 protein expression in gastrocnemius muscles. (*A*) A representative Western blot analysis of the expression of TRPC3, TRPC6, and glyceraldehyde-3-phosphate dehydrogenase in the gastrocnemius muscle from wild-type, wild-type/dominant-negative TRPC6, *RYR1*-p.R163C, and *RYR1*-p.R163C/dominant-negative TRPC6 mice. (*B*) Summary of the densitometric analysis. The data were normalized to glyceraldehyde-3-phosphate dehydrogenase and expressed as mean optical unit values ± SD. Three mice per genotype. For TRPC3 and TRPC6 protein expression, the densitometric quantitative data were based on three independent experiments from each mouse. The values are expressed as means ± SD for each condition. Statistical analysis was done using unpaired Student's independent *t* test. $*P \leq 0.05$.